Biomaterials Science

ARTICLE

Gold nanoparticle interactions with endothelial cells cultured under physiological conditions

Received 00th January 20xx,
Accepted 00th January 20xx

DOI: 10.1039/x0xx00000x

www.rsc.org/

C. Freese[a*], L. Anspach[a], R. C. Deller[b]†, S.-J. Richards[b], M. I. Gibson[b], C. J. Kirkpatrick[a] and R. E. Unger[a]

PEGylated gold nanoparticles (AuNPs) have an extended circulation time after intravenous injection *in vivo* and exhibit favorable properties for biosensing, diagnostic imaging, and cancer treatment. No impact of PEGylated AuNPs on the barrier forming properties of endothelial cells (ECs) has been reported, but recent studies demonstrated that unexpected effects on erythrocytes are observed. Almost all studies to date have been with static-cultured ECs. Herein, ECs maintained under physiological cyclic stretch and flow conditions and used to generate a blood-brain barrier model were exposed to 20 nm PEGylated AuNPs. An evaluation of toxic effects, cell stress, the release profile of pro-inflammatory cytokines, and blood-brain barrier properties showed that even under physiological conditions no obvious effects of PEGylated AuNPs on ECs were observed. These findings suggest that 20 nm-sized, PEGylated AuNPs may be a useful tool for biomedical applications, as they do not affect the normal function of healthy ECs after entering the blood stream.

Introduction

Specific physico-chemical properties make inorganic nanoparticles such as gold nanoparticles (AuNP) versatile tools for biomedical applications, which include biosensing, diagnostic imaging and cancer treatment.[1,2] The inert character of gold, the easy and reproducible synthesis as well as the ease of functionalization with thiol-coating ligands make this desirable for a variety of applications. A number of studies with AuNPs have shown that size, shape, concentration, and surface modification of the NPs affect the interaction with cells and may lead to varying degrees of internalization and cytotoxicity.[3–6] Modifying the surface of AuNPs with polyethylene glycol (PEG) has been demonstrated to prolong the circulation time in vivo,[7,8] this being explained by a reduced renal filtration[9] In addition, it has been demonstrated that 15 nm PEGylated AuNPs do not affect platelet aggregation, nor do they induce pro-inflammatory cytokines in endothelial cells.[10] In previous studies it was also shown that PEGylated AuNPs of different sizes did not reduce cell viability or induce cellular stress and were internalized in low amounts by various microvascular endothelial cells compared to the same AuNPs functionalized with various surface polymers.[6,11] However, some studies have shown that AuNPs covered with PEG have a negative impact on cells and organisms. As demonstrated by Huang and colleagues 6.1 nm-sized PEGylated AuNPs were able to induce apoptosis of human chronic myeloid leukemia K562 cells.[12] In addition to these *in vitro* results Cho *et al.* showed that treatment with 13 nm PEGylated AuNPs led to apoptotic effects in the liver of mice.[13] Furthermore, He *et al.* also showed that PEGylated AuNPs had a negative impact on the function of human erythrocytes.[14] Based on these contradictory results of the effects of PEGylated AuNPs on cells and organs we decided to use more biologically relevant *in vitro* culture conditions to analyse the effect of PEGylated AuNPs on ECs *in vitro*.

The endothelium plays a pivotal role in the homeostasis of tissues and small changes in the function of ECs might impact the functionality of organs or even the health of an entire organism.[15] In addition to examining toxic effects, an evaluation of PEGylated AuNPs on EC pro-inflammatory induction is necessary. An increased expression of cell adhesion molecules leads to leukocyte adhesion to the activated endothelium and results in transmigration into the tissue. To evaluate these parameters, three different model systems that differ from the traditional monocultures on tissue culture plastic were used. Since blood flow has been demonstrated to be important for endothelial differentiation and function,[16–18] ECs were cultured under flow conditions and the morphology and cellular functions of ECs after the treatment with PEGylated AuNP were compared to cells grown under static conditions. In addition to flow, the impact of

[a] *REPAIR-lab, Institute of Pathology, University Medical Center of the Johannes Gutenberg University Mainz and European Institute of Excellence on Tissue Engineering and Regenerative Medicine, Langenbeckstr. 1, 55131 Mainz, Germany.*
[b] *University of Warwick, Department of Chemistry, Coventry, CV4 7AL, United Kingdom.*
* *corresponding author: freesec@uni-mainz.de*
† current address: University of Bristol, School of Cellular and Molecular Medicine, Bristol, BS8 1TD, United Kingdom
Electronic Supplementary Information (ESI) available: : Supplemental figure 1. Characterization of PEGylated gold nanoparticles Supplemental figure 2. E-selectin expression in HUVEC after AuNP exposure Supplemental figure 3. HUVEC cultured under flow conditions. See DOI: 10.1039/x0xx00000x

stretch, which is also an important stimulus for EC function, was evaluated to determine how nanoparticles interact and influence cells under these conditions. We have previously shown that silica NPs interact differently with ECs under stretch compared to static culture conditions.[19] The present study aims at determining if a changed nanoparticle-cell interaction is observed by comparing static to flow or stretch culture conditions and whether these conditions result in changes to the induction of cytotoxicity or pro-inflammatory effects in the presence of PEGylated AuNPs or whether the uptake behaviour of the NPs into cells is altered. The third model system is based on an *in vitro* blood-brain barrier (BBB) co-culture model previously described.[20,21] Since the brain is protected by a specific differentiated endothelium that in concert with other cell types generates the neurovascular unit and protects the brain from xenobiotic substances,[22,23] this model was used to determine if the synthesized PEGylated AuNPs impact the BBB. Thus, the integrity, the metabolic activity and the induction of cytokine expression of brain endothelial cells were also examined. Moreover, the transport properties across the barrier were determined using inductively coupled plasma and optical emission spectroscopy (ICP-OES). Due to the many promising biomedical applications of PEGylated AuNPs and to confirm the inert character of PEGylated AuNPs, this *in vitro* study was performed to investigate the impact of 20 nm PEGylated AuNPs on primary ECs by using more biologically relevant cell culture models and conditions.

Experimental

Nanoparticle synthesis and characterization

Gold(III) chloride trihydrate ($HAuCl_4$; > 49 % Au, ACS grade) and poly(ethylene glycol) 2-mercaptoethyl ether acetic acid (M_n = 3500 $g.mol^{-1}$) were purchased from Sigma-Aldrich. Tri-sodium citrate (99.8 %) was purchased from Acros Organics. Ultrahigh quality water with a resistance of 18.2 MΩ x cm (at 25°C) was obtained from a Millipore Milli-Q gradient machine fitted with a 0.22 µm filter. 20 nm PEGylated gold nanoparticles were synthesized as followed. First, 600 mL of a 0.85 mmol / L (0.33 mg / mL) aqueous solution of $HAuCl_4$ was heated to reflux in a scratch-free round bottomed flask. After that, 10.5 mL of a 0.5 mol / L aqueous solution of sodium citrate was added to the $HAuCl_4$ solution to give an Au : citrate ratio of 1 : 3.5. The temperature was maintained at reflux for 30 minutes, during which time a deep red coloration formed. The reaction mixture was then allowed to cool to room temperature over a period of 3 hours. AuNP PEGylation was performed by the addition of 5 mg 3.5 kDa poly(ethylene glycol) 2-mercaptoethyl ether acetic acid to 20 mL of 1 OD AuNPs for a period of 2 hours at room temperature prior to washing four times with milli-Q water by centrifugation at 16000 x g for 15 minutes at room temperature. On the final wash the resulting supernatant was discarded and replaced with 5 mL of 100 mM MES buffer (pH 5). Particle size analysis was determined by dynamic light scattering using a Malvern Zetasizer Nano ZS instrument. A 4 mW He-Ne 633 nm laser module was used and scattered light was measured at 173° (back scattering). The attenuator and position was selected automatically by the instrument and particle sizes reported as the average of 4 measurements. UV-visible spectra were obtained using a Biotech Synergy HT and processed using the Gen5 software package.

Isolation of HUVECs and assessment of cytotoxicity

Umbilical cords were obtained from randomly selected healthy mothers. Human umbilical vein endothelial cells (HUVEC) were isolated according to a previously published method[24] and cultured on gelatin-coated culture flasks using endothelial cell basal medium (ECBM; PromoCell), 15 % fetal calf serum, 2.5 ng / mL basal fibroblast growth factor, 10 µg / mL sodium heparin (all Sigma-Aldrich) and 100 U penicillin and 100 mg / mL streptomycin (hereinafter referred to as ECBM culture medium) and used until passage 3. For experiments cells were seeded onto fibronectin-coated 96-well plates in ECBM culture medium and cultured to confluence. Cells were exposed to various concentrations of AuNPs for various time points. The AuNPs were diluted in ECBM, supplement mix (PromoCell) and 100 U penicillin and 100 mg / mL streptomycin (hereinafter referred to ECBM stimulation medium). Cell viability was measured using the CellTiter 96 AQueous non-radioactive assay (Promega) as recommended by the manufacturer. For the detection of cytotoxicity caused by the treatment of AuNPs, 50 µL of the cell supernatant was used to carry out the CytoTox 96 non-radioactive cytotoxicity assay (Promega). As a positive control cells were lysed with 1 % TritonX 100 (Sigma-Aldrich) in ECBM and set as 100 % LDH release. Control cells which have been treated with the appropriate volume of nanoparticle diluent were used to determine the basal level of LDH release. After measuring cell viability cells were washed with phosphate-buffered saline (PBS) and fixed with methanol / ethanol (2:1 (v / v)) at room temperature for 15 minutes and used for crystal violet staining or E-selectin determination by cell adhesion molecule enzyme immunoassay (CAM-EIA). Cells were incubated with 100 µL 0.1 % crystal violet solution at room temperature for 20 minutes. Afterwards excess of crystal violet was removed by washing the cells with water. The culture plates were dried and the bound crystal violet was dissolved by adding 60 µL acetic acid. The absorbance of the solution was measured at a wavelength of 600 nm using a multiplate reader (TECAN). E-selectin CAM-EIA was performed as previously described to evaluate AuNPs as an initial screen for presence of endotoxin.[25] Cells treated with 1 µg / mL lipopolysaccharide (LPS) was used as positive control and set as 100 % E-selectin expression.

Uptake of AuNPs into primary endothelial cells

HUVECs were seeded onto fibronectin-coated µ-slides (Ibidi) and cultured in ECBM culture medium until confluence. Cells were treated with 25 µg / mL AuNP in ECBM stimulation medium for 24 hours, washed, fixed with paraformaldehyde and stained with anti-CD31 antibody (DakoCytomation) as

described previously.[26] Images were collected using a fluorescent microscope (Olympus IX71 with Delta Vision system, Applied Precision, USA).

Nanoparticle treatment during cyclic stretch

HUVECs were cultured on fibronectin-coated flexible silicon membranes (BioFlex Culture Plate (FlexCell International Corporation)) with ECBM culture medium and exposed to cyclic stretch (5 % elongation (sinus), 1 Hz) using a FX-4000 Tension Plus FlexerCell strain unit and a FlexLink controller as described previously.[19] After 24 hours of PEGylated AuNP treatment (25 µg / mL) supernatants were collected for ELISA and cells were fixed and stained as describe above. For quantification, cells were washed twice with PBS and collected in tubes after detachment with trypsin/EDTA (Gibco) solution.

Nanoparticle treatment under flow condition

HUVECs were seeded onto fibronectin-coated µ-Slide VI 0.1 flow chambers (Ibidi) and cultured in ECBM culture medium. After 24 hours cell culture medium was changed to remove detached cells. The flow chamber was connected to the pump system consisting of the ibidi pump, the fluidic unit and controlled by the computer pump system. Shear stress was progressively increased up to 15 dyn / cm² starting with 7, to 9, to 11 dyn / cm² for 6 hours each. After 48 hours of flow the cells were incubated with PEGylated AuNPs for 24 hours under flow conditions using 25 µg / mL PEGylated AuNPs diluted in ECBM stimulation medium. The medium of the static controls was changed every day and stimulated with the same nanoparticle stock solution for 24 hours under static culture conditions.

In vitro blood-brain barrier model

Porcine brain endothelial cells (PBEC) were isolated and co-cultured with SH-SY5Y cells as described previously.[20,21] At day 8 after seeding of PBECs, SH-SY5Y cells were seeded in the wells below the PBECs. After 24 hours of co-cultivation with SH-SY5Y cells, PBECs were treated with 12.5 and 25 µg / mL PEGylated AuNPs. For the treatment 20 µL of the supernatant was removed and 20 µL of PEGylated AuNPs and sodium fluorescein (NaFITC) was added. The transendothelial electrical resistance (TEER) was measured before and after 24 hours of nanoparticle exposure. In addition 50 µL of the supernatant from the lower compartment was transferred to a 96 well plate and fluorescence was measured (Ex 485 nm, Em 525 nm) to calculate the permeability coefficient of NaFITC as described previously.[20] The medium above the cells was collected and used for the analysis of secreted IL-8 using the porcine ELISA (DuoSet, R&D Systems). For the determination of cell viability PBECs were washed with PBS and incubated with diluted MTS reagent (CellTiter 96 AQueous non-radioactive assay; Promega). After an incubation of 1 hour the absorbance was measured at 492 nm. For the staining procedure cells were washed with PBS and fixed with EtOH / MetOH (1:2 (v / v)) at room temperature for 20 minutes. Claudin-5 was stained as described previously using anti-claudin-5 (abcam).[20] Fluorescent images were collected using the fluorescent microscope BZ9000 (Keyence). For quantification of internalized PEGylated AuNPs PBECs were washed with PBS and collected after trypsination. In addition to the PBECs, the supernatant below the PBECs were analysed for the amount of transported PEGylated AuNPs across the *in vitro* BBB model system (see ICP-OES).

Enzyme- linked immunosorbent assay (ELISA)

After exposure to the PEGylated AuNPs under different culture conditions the supernatants of the cells were diluted in the appropriate assay diluent and analysed via ELISA (DuoSet, R&D Systems) for secreted soluble pro-inflammatory mediators (sVCAM, IL-8, MCP-1) as recommended by the manufacturer. To analyse the supernatant of the PBEC for IL-8 secretion the porcine IL-8 ELISA was used (DuoSet, R&D Systems).

Inductively coupled plasma optical emission spectroscopy (ICP-OES)

To quantify the amount of gold within cells or in supernatants samples were prepared as described previously.[27] Briefly, samples of 200 µL were treated with 150 µL of aqua regia (3:1 hydrochloric acid : nitric acid (both purchased from Fisher Scientific)) at room temperature overnight. All samples were further diluted with 5 mL using MilliQ water to give a total sample volume of 5.35 mL. These samples were then analysed for total gold content by inductively coupled plasma optical emission spectroscopy (ICP-OES; Perkin Elmer Optima 5300DV), and the measurement was repeated 3 times at a wavelength of 267.6 nm for each sample.

Determination of RNA quality and Real-time Polymerase chain reaction (PCR)

Cells were lysed with RLT buffer containing 1 % β-mercaptoethanol. RNA was isolated using RNeasy Midi Kit (Qiagen) as described by the manufacturer. The amount of RNA in each sample was measured with the NanoDrop ND1000 spectrophotometer. To investigate the quality of the RNA the RNA integrity number (RIN) was determined by using Agilent Bioanalyzer and Agilent RNA 6000 Pico Kit. RNA with a RIN ≥ 9.7 was used for quantitative real-time PCR. 1 µg of RNA was used for the reverse transcription polymerase chain reaction according to a standard protocol using Omniscript RT kit (Qiagen). For the quantitative real-time PCR 4 ng cDNA was amplified using 12.5 µL of Power SYBR® Green PCR Master Mix (Applied Biosystems) and 100 nM of each primer in each reaction. Quantitative real-time PCR was performed in triplicate with the 7300 Real-time PCR System (Applied Biosystems) using the following cycler program: 95°C, 15 min; denaturation step: 94°C; 15 s; annealing step: 60°C 30 s; elongation step: 72°C 35 s; dissociation: 95°C 15 s; 60°C 1 min; 95°C 15 s; 40 cycles were performed in total. Ribosomal protein L13a (RPL13A) was used as an endogenous control to calculate ΔΔct.

Polymerase chain reaction

10 ng cDNA were amplified by PCR with specific primer pairs (1 µM each), and a master mix containing 14.875 µl RNAse-free water, 2.5 µL 10-fold buffer, 0.5 µl 2' deoxyribonucleotides (dNTP) mix, and 0.125 µL Taq DNA polymerase (Taq PCR Core Kit, Qiagen). PCR was performed using PCR System 9700 cycler, 35 cycles and the following

cycler program: 94°C, 2 min; 94°C, 0.5 min; 58°C, 0.5 min; 72°C, 0.5 min; 72°C, 10 min. PCR products were separated by gel electrophoresis in a 3 % agarose gel including 0.02 % ethidium bromide and Tris/Borate/EDTA buffer (TBE). Images were obtained using a digital camera.

Sequences of oligonucleotides used for PCR and real-time PCR

Xbp1unspliced: 5'-CAGACTACGTGCACCTCTGC-3'; 5'-CTTCTGGGTAGACCTCTGGG-3', Xbp1 spliced: 5'-TCTGCTGAGTCCGCAGCAGG-3'; 5'-CTTCTGGGTAGACCTCTGGG-3', Xbp1u/s: 5'-CTGGAACAGCAAGTGGTAGA-3'; 5'-CTGGGTCCTTCTGGGTAGAC-3', BiP: 5'-ACTATGAAGCCCGTCCAGAAAGT-3'; 5'-TCGAGCCACCAACAAGAACA-3'

Statistical analyses

One-way ANOVA with various post-test analyses were performed using GraphPad Prism version 5.04 software for Windows, GraphPad Software, San Diego California USA, www.graphpad.com. The specific post-test and the number of donors are indicated in the figure legends. Significances are shown by asterisks, while $P < 0.05$, $P < 0.01$, and $P < 0.001$ are indicated by *, **, and ***, respectively.

Results and Discussion

Nanoparticle interaction with cells has to be analysed in detail for every unique nanoparticle. In this study, 20 nm PEGylated AuNPs are used. These were prepared by a standard ligand exchange process using thiolated PEG and citrate-stabilized gold particles.[28] The resulting particles were characterized by dynamic light scattering (DLS) and UV / Vis spectroscopy (UV-Vis), as shown in Supplemental figure 1. Upon functionalization with the PEG, the particle size increased slightly to 30 nm and displayed a small shift in the surface plasmon resonance band, indicative of a successful functionalization. The particles were also stable in various media, including PBS and cell culture media, thus confirming that the PEG coating stabilizes the particles and prevents non-specific adhesion of biomolecules.

As a next step the nanoparticle suspension was analysed for a potential contamination with bacterial endotoxin to avoid the misinterpretation of cytokine release of endothelial cells following PEGylated AuNP treatment. As shown in Supplemental figure 2 none of the investigated PEGylated AuNP concentrations led to an upregulation of E-selectin in primary human endothelial cells compared to the untreated control. Thus, contamination with bacterial endotoxin could be excluded since this assay system was evaluated to be highly sensitive for the detection of endotoxin, as demonstrated by Unger *et al.*.[25]

After the characterization of the PEGylated AuNPs the impact of the nanoparticles on primary ECs (HUVEC) was determined. In Figure 1 A the results show that concentrations of PEGylated AuNPs up to 100 µg / mL were not toxic to HUVEC (as adjudged by the release of lactate dehydrogenase). In addition, the metabolic activity was not reduced in cells that were treated with a high dose of nanoparticles (Figure 1 B). These results were in agreement to previously published data by our group, which showed that 18 nm, 35 nm, and 65 nm PEGylated AuNPs were not toxic to human primary dermal microvascular endothelial cells or to brain microvascular endothelial cells.[6,11] In addition, in vitro studies by other groups generally showed only a slight effect of PEGylated AuNPs on various cell types (alveolar type II cells, macrophages, microglia).[29–31] However, the cell proliferation measured by the expression of the proliferation factor Ki-67 was inhibited to 60 % when the cells were exposed to 100 µg / mL PEGylated AuNPs for 24 hours (Figure 1 C). These data were supported by the determination of the cell number that was also reduced to 62 % compared to control cells under these conditions (Figure 1 D).

Figure 1. Determination of cell biocompatibility of 20 nm PEGylated gold nanoparticles.

HUVECs were treated with PEGylated AuNPs on cell culture dishes for 24 hours. (A) Cytotoxicity was determined by LDH-assay and data were normalized to lysed cells. (B) The MTS-Assay was used to determine cell viability and the acquired data were normalized to the untreated control expressed in %. (C) The proliferation was detected by measuring the proliferation factor Ki-67, while the cell number was determined using crystal violet staining (D). Results shown are means ± SD calculated using the results of at least three independent experiments. *: $P < 0.05$, **: $P > 0.01$; ***: $P < 0.001$ compared to the appropriate untreated control (ONEway ANOVA with Dunnetts t-test; n = 2-7). (E, F) Merged images of HUVEC cultured on plastic dishes (E) and additionally treated with gold nanoparticles (F). Staining of CD31 (red) expressed in HUVEC, nuclei in blue and DIC, scale bars: 15 µm.

The decreased proliferation rate after exposure to a high dose of PEGylated AuNPs is in agreement with the results observed in previous studies.[27] Based on the cell viability determined in the various assays, NP concentrations of 12.5 to 25 µg / mL were used in further studies. The images presented in Figure 1 E and F demonstrate that the exposure to 25µg / mL AuNPs did not affect the cell morphology of HUVEC and did not reduce or change the expression of CD31, a membrane-bound adhesion molecule, compared to the untreated control. These results demonstrated that PEGylated AuNPs applied to cells cultured under normal static cell culture conditions were not toxic and did not affect adhesion molecule expression by the cells.

Contradictory results have been observed by He *et al.,* who focused on the function of erythrocytes exposed to PEGylated AuNPs.[14] They showed an unexpected reduction of oxygen-delivering ability, a shortened lifetime of erythrocytes and a decreased expression of CD47 after AuNP exposure. Based on this, the potential impact of PEGylated AuNPs on endothelial cells was examined using more biologically relevant *in vitro* cell culture models to analyze the interaction of PEGylated AuNPs and endothelial cells under conditions closely mimicking the *in vivo* situation.

Since it was shown that shear stress regulates EC function and differentiation,[16,32] and enhanced the accumulation of liposomes targeted to vascular cell adhesion molecule- (VCAM-) 1 and also non-targeted nanoparticles in endothelial cells,[32,33] nanoparticle-cell interactions were explored under physiological medium flow conditions. The cartoon in Figure 2 A shows the movement of the added NPs across the cells under flow conditions. Cells were initially cultured for 48 hours

under flow, after which they were exposed to nanoparticles for a further 24 hours under flow conditions.

Figure 2. Treatment of HUVEC with 20 nm PEGylated gold nanoparticles under flow culture conditions.

(A) Cartoon of the flow culture model system (15 dyn / cm²). (B) Immunofluorescent images of HUVEC under flow culture conditions without (i) or exposed to gold nanoparticles (ii). Staining of CD31 (green) expressed in HUVEC, nuclei in blue, scale bars: 100 µm. (C) Quantification of internalized gold in HUVEC under static or flow culture conditions determined using ICP-OES (n = 6).

The images in Figure 2 B i and ii show that the PEGylated AuNPs had no impact on the morphology of ECs. In addition, the amount of PEGylated AuNPs internalized by the cells was quantified using ICP-OES and compared to the uptake behaviour observed under static cell culture conditions (Figure 2 C). Although the morphology of HUVECs changed after the application of shear stress (Supplemental figure 3), the internalization of PEGylated AuNPs was very low under both culture conditions (Figure 2 C). As PEGylation of nanoparticles was demonstrated to prolong the circulation time in blood [7,8] and also delayed or even prevented the internalization into cells [6,34,35], the results of the flow experiments presented were in accordance with results previously described. In addition, the uptake of PEGylated AuNPs was very low; an altered internalization rate for the PEGylated AuNPs could be detected in cells cultured under static or flow conditions. This is also in agreement with the data previously published by Fede *et al.* who detected the same tendency for the internalization of AuNPs (w/o PEG) in HUVEC under static and flow conditions using a microfluidic system.[36]

In addition to shear stress, cyclic stretch is also a prominent hemodynamic force which acts on endothelial cell function and membrane traffic[17,37] and may alter the internalization of nanoparticles in endothelial cells. As previously reported, we showed that stretch affects the interaction of endothelial cells with amorphous silica nanoparticles and leads to a reduced internalization.[19] In contrast, studies by Rouse *et al.* demonstrated an increased interaction of quantum dots with keratinocytes under stretch compared to static cell culture conditions.[38] Thus, studies were carried out to determine if PEGylated AuNPs are internalized in different amounts in endothelial cells when cultured under stretch conditions

Figure 3. Impact of 20 nm PEGylated AuNPs on HUVEC cultured under physiological stretch conditions.

(A) Cartoon of the stretch model system (5 % stretch, 1 Hz). (B) Immunofluorescent images of HUVEC exposed to gold nanoparticles under static (i – iii) or stretch (iv – vi) culture conditions. Staining of CD31 (green) expressed in HUVEC (i + iv) and DIC images (ii + v); overlays in (iii) and (vi). Scale bars: 15 µm. (C) Secretion of interleukin-8 (IL-8), soluble vascular cell adhesion molecule (sVCAM), and monocyte chemoattractant protein-1 (MCP-1) after AuNP exposure under static (s) or stretch/flex (f) culture conditions measured by ELISA. LPS treatment was used as a positive control (n = 3-6). (D) PCR detecting spliced and unspliced Xbp1 mRNA via separation using a 3 % agarose gel. Actin was used as reference gene. (E) Quantitative real-time PCR for investigation of BiP, unspliced (Xbp1u) and spliced (Xbp1s) Xbp1 mRNA expression. Results are depicted as relative quantification (RQ) (n=2). (F) Quantification of BiP expression on protein level detected by Western Blot shown as X-fold change of static control (n=4). (G) Quantification of internalized gold in HUVEC under static or stretch culture conditions determined using ICP-OES (n=3).

(Figure 3 A) and whether these culture conditions together with nanoparticles had any impact on cell function or morphology. In Figure 3 B the morphology of the cells after exposure to the nanoparticles under static (i – iii) and stretch (iv – vi) conditions is shown. Differences in the morphology could not be detected. Since agglomerates of internalized PEGylated AuNPs can also be detected by light microscopy,[6] the cells treated with AuNPs under both culture conditions were analysed using microscopy. However, no agglomerates of PEGylated AuNPs were visible within the cells (ii, v). In addition to the microscopic images, the quantification by ICP-OES indicated low levels of PEGylated AuNPs within the cells (Figure 3 G). In addition to the cellular uptake and changes in morphology the release of pro-inflammatory mediators after NP treatment in the stretch model system was examined. Based on the results previously reported by Santos-Martinez *et al.* that no induction of inflammatory response in endothelial cells after AuNP exposure was detectable, no release of cytokines by endothelial cells was expected in the stretch culture system.[10] Moreover, Kim *et al.* could not identify any inflammation in the retina of C57BL/6 mice.[39] Nevertheless, results from *in vivo* studies showed that inflammation of the liver after exposure to PEGylated AuNPs was present.[13] Since endothelial cells are important for the homeostasis of tissues and organs and also play a crucial role in inflammation processes, the release of pro-inflammatory mediators after exposure to PEGylated AuNPs under the different culture conditions were analysed in the present *in vitro* study (Figure 3 C). The results demonstrated that untreated control cells release a basic level of interleukin-8 (IL-8) under both culture conditions and that the level of IL-8 is slightly increased after the exposure to the NPs. However, no significant differences between the two culture conditions and the nanoparticle exposure in parallel were detected but the treatment with lipopolysaccharide (LPS) as positive control resulted in a 10-fold increase of secretion of IL-8. These observations are mirrored by the secretion of monocyte chemoattractant protein-1 (MCP-1). Moreover, no soluble (s) VCAM was detected in the supernatant of untreated control cells and NP-treated cells, either under static or under stretch culture conditions. In summary, no significant induction of inflammation processes were detected in ECs in the stretch model system compared to the LPS-treated endothelial cells.

In addition to the analyses of the induction of pro-inflammatory factors we also examined whether cell stress might occur in ECs after exposure to nanoparticles. Several studies have previously shown induced endoplasmic reticulum (ER) stress in different cell types after treatment with silver-doped silica NPs,[40] silver NPs[41,42] or polystyrene nanospheres.[43] Chen *et al.* showed that zinc oxide NPs triggered ER stress in HUVEC[44] and gold NPs were shown to induce stress signaling in K562 cells.[45] However, previous studies show that AuNPs of three different sizes and four

surface modifications did not cause any ER stress in brain endothelial cells.[11] In general, ER stress is measurable by the detection of ER stress markers, which constitute components of the Unfolded Protein Response (UPR). Activating the signalling pathway UPR, the cells react on ER stress and begin to counteract the stress situation. In the event that a cell cannot restore homeostasis, apoptosis will be induced.[46] Thus, activation of the UPR presents an early and sensitive marker for toxic potential of NPs. The expression of the UPR component chaperone BiP and splicing of xbp1 mRNA was determined in HUVEC under static and stretch cell culture conditions and in the presence or absence of the nanoparticles. Fig. 3 D shows the detection of unspliced and spliced form of xbp1 mRNA determined by PCR. Neither exposure of the cells to NP nor the different culture conditions led to splicing of xbp1 mRNA. In addition, real-time PCR studies examining xbp1 splicing demonstrated no differences between unspliced and the spliced form of the transcription factor mRNA (Fig. 3 E). Furthermore, expression of BiP at the mRNA level was not increased after NP treatment. A slight increase of BiP, xbp1u and xbp1s mRNA was detected under stretch culture conditions. However, these changes were neither numerically large nor statistically significant. In addition, we investigated the expression of the ER stress marker BiP at the protein level by Western Blot analysis. Quantification of BiP expression (Fig. 3 F) showed a minor but non-significant decrease of BiP expression as a result of PEGylated AuNP treatment. Changes in expression due to static and stretch culture conditions were not observed. In summary, treatment with PEGylated AuNPs did not lead to ER stress and UPR activation in HUVEC under static, as well as stretch culture conditions. This kind of stress resistance of HUVEC to AgNPs has been previously described by Huo *et al*..[42]

In addition to the hemodynamic forces that alter the phenotype of endothelial cells and may also effect nanoparticle-cell interactions, whether the barrier function of endothelial cells is influenced during nanoparticle exposure is also of great importance. In particular, capillary endothelial cells in the brain form a very tight barrier which protects the brain from endobiotic and xenobiotic substances.[23] In order to examine this, a well-characterized blood-brain barrier model was used to determine whether the barrier function is influenced during exposure to PEGylated AuNPs (Figure 4 A).[20,21]

Figure 4. Assessment of the impact of 20 nm PEGylated AuNPs on endothelial cells forming the blood-brain barrier.

(A) Cartoon of the blood-brain barrier co-culture model. (B) The MTS-Assay was used to determine cell viability after 24 hours of exposure to PEGylated AuNPs and the acquired data were normalized to the untreated control expressed in % (n = 3 - 4). (C) Immunofluorescence staining of claudin-5 proteins (green) expressed in PBEC without PEGylated AuNPs (i) or after PEGylated AuNPs treatment (ii). Nuclei in blue, scale bars: 200 µm. (D) Transendothelial electrical resistance (TEER) was measured before and after the exposure to gold nanoparticles for 24 hours. Ctrl was treated with the corresponding volume of diluent. Data represent the mean ± standard deviation of four experiments. Cells with at least 170 Ohm x cm² were used (n = 4 - 5). (E) To ensure the tightness of the barrier during the treatment with PEGylated AuNPs, the permeability coefficient of sodium fluorescein was simultaneously determined (n = 2). (F) Quantification of transported gold across the PBEC barrier using ICP-OES (n = 3). (G) Secretion of interleukin-8 from PBECs during PEGylated AuNP treatment was compared to the untreated control (n = 2 - 6).

The blood-brain barrier model was exposed to nanoparticle (12.5 µg / mL and 25 µg / mL) to evaluate the impact on the metabolism of brain endothelial cells. The results of the viability assay shown in Figure 4 B demonstrate that exposure to the two concentrations of NP had no impact on the primary porcine brain microvascular endothelial cells (PBECs). Also, no changes to the cell morphology or to cell-cell contacts were observed during exposure to PEGylated AuNPs. This was shown by the staining of the tight junction protein claudin-5 (Figure 4 C). Moreover, the levels of the transendothelial electrical resistance (TEER) demonstrated that the tight junctions were not affected by NP exposure (Figure 4 D). The integrity of the barrier was also determined based on the permeability of the model substance sodium fluorescein. The permeability coefficient of untreated and NP-exposed cells was determined and compared (Figure 4 E). No differences were observed in the permeability coefficient between NP-exposed and control cells. Thus, based on the results obtained by the measurement of the TEER and the sodium fluorescein permeability results we can conclude that the barrier function of the endothelial cells was not altered when exposed to the 20 nm PEGylated AuNPs. The amount of PEGylated AuNPs transported across the endothelial cell layer was also determined. The ICP-OES data illustrated in Figure 4 F show that the AuNPs were not transported across the cell barrier. In addition, the PEGylated NPs did not induce any inflammatory response in the PBECs even at a dose of 25 µg / mL PEGylated AuNPs (Figure 4 G). Recently published data by the Trickler group also demonstrated that PBEC did not secrete inflammatory mediators in response to exposure to 5 nm AuNPs.[47] This group also showed no changes in barrier integrity, the absence of cytotoxicity and no induction of inflammatory cytokines in rat brain microvascular endothelial cells exposed to the 5 nm AuNPs, similar to the results observed in the present studies with porcine brain endothelial cells and the 20 nm PEGylated AuNPs.[48]

Taken together, the results of this study indicate that PEGylated gold nanoparticles did not impact peripheral endothelial cells evaluated in two physiological hemodynamic model systems. Moreover, the healthy blood-brain barrier is not affected by PEGylated AuNPs. In contrast Etame *et al.* previously showed by using a transport-permissive brain microvasculature model system that optimizing the size of AuNPs and the length of the PEG chain results in a transport of AuNPs across the brain microvasculature. They proposed that such modified AuNPs might be transported across the barrier into the brain tissue or possibly into malignant brain tumors.[49] In addition, it has been shown that the application of PEGylated AuNPs resulted in a significant decrease in cancer cell survival after gamma radiation *in vitro* and that AuNPs accumulated in high concentrations in tumors while also decreasing tumor volume *in vivo*.[50] These results ultimately

lead to the conclusion that PEGylated AuNPs might be useful as nanotools for improved radiotherapy while not affecting peripheral and healthy brain endothelial cells or the integrity of the BBB.

Nevertheless, previous studies have also demonstrated that AuNPs have an impact on both liver and kidney in mice,[13] indicating that these NPs need to be carefully evaluated prior to future medical applications. However, PEGylated AuNPs have a number of positive properties as demonstrated by several studies. Modifying the surface of the NPs with an additional targeting protein/sequence may reduce the side effects causing liver impairment. However, each uniquely-modified AuNP needs to be evaluated prior to use in medical applications. Thus, by using the more complex *in vitro* models described in the present study which mimic the *in vivo* situation, a more biologically relevant evaluation of novel NPs can be obtained and the most effective NPs can be selected for further animal studies. However, even though these model systems lead to a more physiological phenotype of endothelial cells, the models cannot completely replace *in vivo* studies. Additional comparative studies between these models with animal studies will be necessary to determine whether the more complex *in vitro* models truly mimic what is observed *in vivo*. Beside the hemodynamic forces, the clearance of nanoparticles by blood cells, the liver, spleen and kidney cannot totally be investigated in *in vitro* experiments and must also be determined. Thus, as stated by Shah and Bischof, *in vitro* experiments are efficient for screening processes but *in vivo* studies are also necessary for confirming the *in vitro* data, especially for blood-nanoparticle interactions.[51]

Conclusions

Cell culture models which more closely reproduce the *in vivo* environment were used to investigate the effects of 20 nm PEGylated AuNPs on endothelial cells (ECs). These culture conditions represent a position between traditional static culture methods and *in vivo* studies by mimicking the stretch and shear-stress that ECs undergo continuously *in vivo*. ECs under these conditions were evaluated using a large panel of assays to probe cellular stress and function. We observed that cells cultured under flow as well as under stretch condition were not affected by the PEGylated AuNPs. No impact on cell morphology, cell viability and no induction of inflammatory or unfolded protein responses (UPR) caused by endoplasmic stress was shown. Even the barrier properties of brain microvascular ECs were affected by the treatment with the 20 nm PEGylated AuNPs. Internalization of the PEGylated AuNPs did not differ significantly between static and flow or stretch condition. In addition the transport across the brain ECs was very low. These more physiological model systems demonstrated that PEGylated AuNPs have many cell-favourable attributes and may be used as a basis in developing a new generation of nanoparticles for medical applications. Moreover, the results from the EC-culture models demonstrate *in vivo*-like characteristics and these models could be a useful addition between traditional static *in vitro* culture studies and *in vivo* toxicity and efficacy studies. As a consequence using these models for NP evaluation studies could reduce animal experiments and drug developmental costs.

Acknowledgements

The authors are grateful to A. Sartoris and B. Pavic for their excellent technical assistance in the cell culture studies. The authors also acknowledge the excellent assistance of Dr. Esther Melo - Herraiz for her help in the equipment setup. Equipment used was supported by the Innovative Uses for Advanced Materials in the Modern World (AM2), with support from Advantage West Midlands (AWM) and part funded by the European Regional Development Fund (ERDF). RCD and SJR acknowledge the EPSRC for studentships from the MOAC Doctoral Training Centre. CF and consumables for the cell culture experiments was partially funded by the FP6 project 'NanoBioPharmaceutics' (NMP4-CT-2006-026723).

Notes and references

Umbilical cords were obtained from randomly selected healthy mothers. All procedures were in agreement with the ethical standards of the University Medical Center of the Johannes Gutenberg-University Mainz (§ 14 AVB, Abs. 3) and with the Helsinki Declaration. Porcine brains were provided by a local butcher (Mainz, Germany) and used with his permission.

(1) E. Boisselier and D. Astruc, *Chem. Soc. Rev*, *2009*, 1759–1782.

(2) A. Majdalawieh, M. C. Kanan, O. El-Kadri and S. M. Kanan, *J Nanosci Nanotechnol*, *2014*, **14**, 4757–4780.

(3) B. D. Chithrani, A. A. Ghazani and W. C. W. Chan, *Nano Letters*, *2006*, **6**, 662–668.

(4) A. M. Alkilany, A. Shatanawi, T. Kurtz, R. B. Caldwell and R. W. Caldwell, *Small*, *2012*, **8**, 1270–1278.

(5) D. Bartczak, O. L. Muskens, S. Nitti, T. Sanchez-Elsner, T. M. Millar and A. G. Kanaras, *Small*, *2012*, **8**, 122–130.

(6) C. Freese, M. I. Gibson, H.-A. Klok, R. E. Unger and C. J. Kirkpatrick, *Biomacromolecules*, *2012*, **13**, 1533–1543.

(7) T. Niidome, M. Yamagata, Y. Okamoto, Y. Akiyama, H. Takahashi, T. Kawano, Y. Katayama and Y. Niidome, *Journal of Controlled Release*, *2006*, **114**, 343–347.

(8) J. Lipka, M. Semmler-Behnke, R. A. Sperling, A. Wenk, S. Takenaka, C. Schleh, T. Kissel, W. J. Parak and W. G. Kreyling, *Biomaterials*, *2010*, **31**, 6574–6581.

(9) Kah, James Chen Yong, K. Y. Wong, K. G. Neoh, J. H. Song, Fu, Jason Wei Ping, S. Mhaisalkar, M. Olivo and Sheppard, Colin James Richard, *J Drug Target*, *2009*, **17**, 181–193.

(10) M. J. Santos-Martinez, K. Rahme, J. J. Corbalan, C. Faulkner, J. D. Holmes, L. Tajber, C. Medina and M. W. Radomski, *J Biomed Nanotechnol*, *2014*, **10**, 1004–1015.

(11) L. Anspach, R. E. Unger, C. Brochhausen, M. I. Gibson, H.-A. Klok, C. J. Kirkpatrick and C. Freese, *Nanotoxicology*, *2016*, **10**, 1341–1350.
(12) Y.-C. Huang, Y.-C. Yang, K.-C. Yang, H.-R. Shieh, T.-Y. Wang, Y. Hwu and Y.-J. Chen, *Biomed Res Int*, *2014*, **2014**, 182353.
(13) W.-S. Cho, M. Cho, J. Jeong, M. Choi, H.-Y. Cho, B. S. Han, S. H. Kim, H. O. Kim, Y. T. Lim, B. H. Chung and J. Jeong, *Toxicology and Applied Pharmacology*, *2009*, 16–24.
(14) Z. He, J. Liu and L. Du, *Nanoscale*, *2014*, **6**, 9017–9024.
(15) W. C. Aird, *Circ. Res.*, *2007*, **100**, 158–173.
(16) N. Azuma, S. Duzgun, M. Ikeda, H. Kito, N. Akasaka, T. Sasajima and B. E. Sumpio, *Journal of Vascular Surgery*, *2000*, **32**, 789–794.
(17) G. Apodaca, *American Journal of Physiology - Renal Physiology*, *2002*, **282**, F179-F190.
(18) R. Estrada, G. A. Giridharan, M.-D. Nguyen, T. J. Roussel, M. Shakeri, V. Parichehreh, S. D. Prabhu and P. Sethu, *Anal. Chem.*, *2011*, **83**, 3170–3177.
(19) C. Freese, D. Schreiner, L. Anspach, C. Bantz, M. Maskos, R. E. Unger and C. Kirkpatrick, *Particle and fibre toxicology*, *2014*, **11**, 1.
(20) C. Freese, S. Reinhardt, G. Hefner, R. E. Unger, C. J. Kirkpatrick, K. Endres and K. M. Iijima, *PLoS ONE*, *2014*, **9**, e91003.
(21) C. Freese, S. Hanada, P. Fallier-Becker, C. J. Kirkpatrick and R. E. Unger, *Microvascular Research*, *2016*, **111**, 1–11.
(22) N. J. Abbott, A. A. K. Patabendige, D. E. M. Dolman, S. R. Yusof and D. J. Begley, *Neurobiology of Disease*, *2010*, 13–25.
(23) N. J. Abbott, D. E. M. Dolman, S. Drndarski and S. M. Fredriksson, *Methods Mol. Biol.*, *2012*, **814**, 415–430.
(24) K. Peters, H. Schmidt, R. E. Unger, M. Otto, G. Kamp and C. J. Kirkpatrick, *Biomaterials*, *2002*, **23**, 3413–3419.
(25) R. E. Unger, K. Peters, A. Sartoris, C. Freese and C. J. Kirkpatrick, *Biomaterials*, *2014*, **35**, 3180–3187.
(26) G. Coué, C. Freese, R. E. Unger, C. James Kirkpatrick and J. F. Engbersen, *Acta Biomaterialia*, *2012,* DOI: 10.1016/j.actbio.2012.12.005.
(27) C. Freese, C. Uboldi, M. I. Gibson, R. E. Unger, B. B. Weksler, I. A. Romero, P.-O. Couraud and C. Kirkpatrick, *Part Fibre Toxicol*, *2012*, **9**, 23.
(28) S.-J. Richards and M. I. Gibson, *ACS Macro Lett*, *2014*, **3**, 1004–1008.
(29) V. Bouzas, T. Haller, N. Hobi, E. Felder, I. Pastoriza-Santos and J. Pérez-Gil, *Nanotoxicology*, *2014*, **8**, 813–823.
(30) E. Hutter, S. Boridy, S. Labrecque, M. Lalancette-Hébert, J. Kriz, F. M. Winnik and D. Maysinger, *ACS Nano*, *2010*, **4**, 2595–2606.
(31) L. Du, X. Miao, H. Jia, Y. Gao, K. Liu, X. Zhang and Y. Liu, *Talanta*, *2012*, **101**, 11–16.
(32) J. Ando and K. Yamamoto, *Circulation Journal*, *2009,* 1983–1992.
(33) J. Kusunose, H. Zhang, M. K. J. Gagnon, T. Pan, S. I. Simon and K. W. Ferrara, *Ann Biomed Eng*, *2013*, **41**, 89–99.
(34) Y. Hao, X. Yang, S. Song, M. Huang, C. He, M. Cui and J. Chen, *Nanotechnology*, *2012*, **23**, 45103.
(35) Samuel, Jain, O'Dowd, Paul, Kashanin, Gerard, Gun'ko, A. Prina-Mello and Volkov, *IJN*, *2012*, 2943.
(36) C. Fede, I. Fortunati, V. Weber, N. Rossetto, F. Bertasi, L. Petrelli, D. Guidolin, R. Signorini, R. de Caro, G. Albertin and C. Ferrante, *Microvascular Research*, *2015*, **97**, 147–155.
(37) M. Anwar, J. Shalhoub, C. Lim, M. Gohel and A. Davies, *J Vasc Res*, *2012*, **49**, 463–478.
(38) J. G. Rouse, C. M. Haslauer, E. G. Loboa and N. A. Monteiro-Riviere, *Toxicology in Vitro*, *2008*, **22**, 491–497.
(39) J. H. Kim, J. H. Kim, K.-W. Kim, M. H. Kim and Y. S. Yu, *Nanotechnology*, *2009*, **20**, 505101.
(40) V. Christen and K. Fent, *Chemosphere*, *2012*, **87**, 423–434.
(41) J.-C. Simard, F. Vallieres, R. de Liz, V. Lavastre and D. Girard, *The Journal of biological chemistry*, *2015*, **290**, 5926–5939.
(42) L. Huo, R. Chen, L. Zhao, X. Shi, R. Bai, D. Long, F. Chen, Y. Zhao, Y.-Z. Chang and C. Chen, *Biomaterials*, *2015*, **61**, 307–315.
(43) H.-W. Chiu, T. Xia, Y.-H. Lee, C.-W. Chen, J.-C. Tsai and Y.-J. Wang, *Nanoscale*, *2015*, **7**, 736–746.
(44) R. Chen, L. Huo, X. Shi, R. Bai, Z. Zhang, Y. Zhao, Y. Chang and C. Chen, *ACS Nano*, *2014*, **8**, 2562–2574.
(45) Y.-Y. Tsai, Y.-H. Huang, Y.-L. Chao, K.-Y. Hu, L.-T. Chin, S.-H. Chou, A.-L. Hour, Y.-D. Yao, C.-S. Tu, Y.-J. Liang, C.-Y. Tsai, H.-Y. Wu, S.-W. Tan and H.-M. Chen, *ACS Nano*, *2011*, **5**, 9354–9369.
(46) J. A. Diehl, S. Y. Fuchs and C. Koumenis, *Gastroenterology*, *2011*, **141**, 38-41, 41.e1-2.
(47) W. J. Trickler, S. M. Lantz, R. C. Murdock, A. M. Schrand, B. L. Robinson, G. D. Newport, J. J. Schlager, S. J. Oldenburg, M. G. Paule, W. Slikker, S. M. Hussain and S. F. Ali, *Nanotoxicology*, *2011*, **5**, 479–492.
(48) W. J. Trickler, S. M. Lantz-McPeak, B. L. Robinson, M. G. Paule, W. Slikker, A. S. Biris, J. J. Schlager, S. M. Hussain, J. Kanungo, C. Gonzalez and S. F. Ali, *Drug Metab. Rev.*, *2014*, **46**, 224–231.
(49) A. B. Etame, C. A. Smith, Chan, Warren C W and J. T. Rutka, *Nanomedicine*, *2011*, **7**, 992–1000.
(50) X.-D. Zhang, Di Wu, X. Shen, J. Chen, Y.-M. Sun, P.-X. Liu and X.-J. Liang, *Biomaterials*, *2012*, **33**, 6408–6419.
(51) N. B. Shah and J. C. Bischof, *BioNanoMaterials*, *2013*, **0**, 1–15.

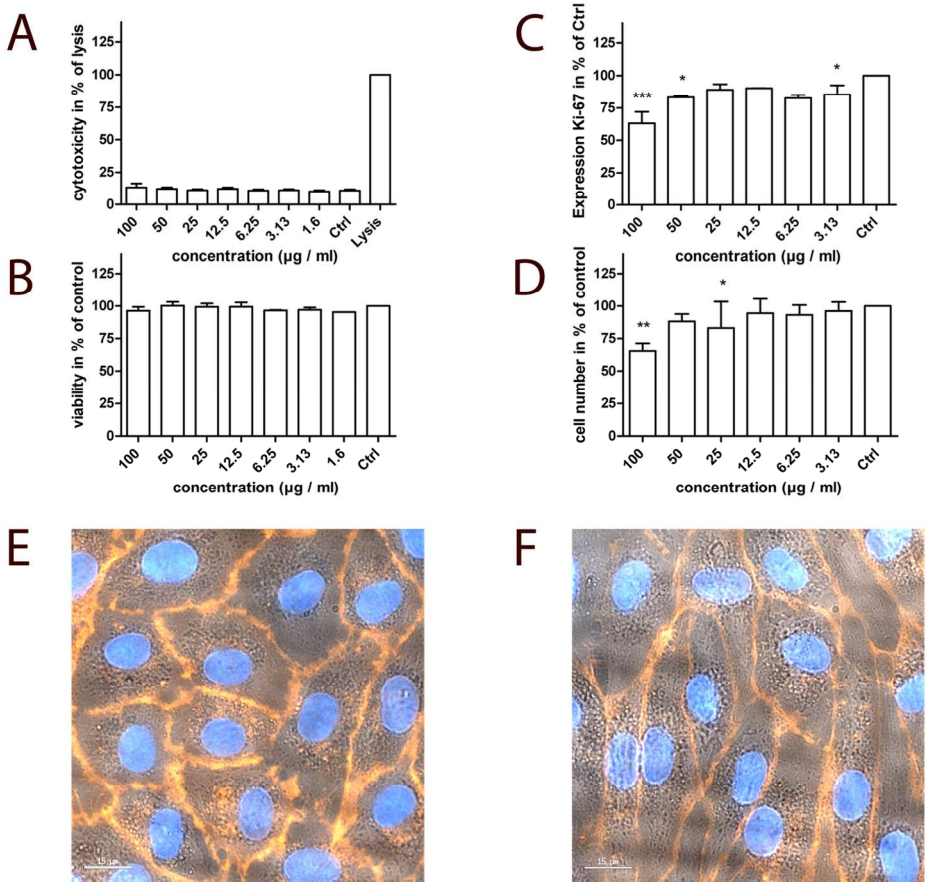

Figure 1. Determination of cell biocompatibility of PEGylated gold nanoparticles.
HUVECs were treated with PEGylated AuNPs on cell culture dishes for 24 hours. (A) Cytotoxicity was determined by LDH-assay and data were normalized to lysed cells. (B) The MTS-Assay was used to determine cell viability and the acquired data were normalized to the untreated control expressed in %. (C) The proliferation was detected by measuring the proliferation factor Ki-67, while the cell number was determined using crystal violet staining (D). Results shown are means ± SD calculated using the results of at least three independent experiments. *: $P < 0.05$, **: $P > 0.01$; ***: $P < 0.001$ compared to the appropriate untreated control (ONEway ANOVA with Dunnetts t-test; n = 2-7). (E, F) Merged images of HUVEC cultured on plastic dishes (E) and additionally treated with gold nanoparticles (F). Staining of CD31 (red) expressed in HUVEC, nuclei in blue and DIC, scale bars: 15 µm.

151x133mm (300 x 300 DPI)

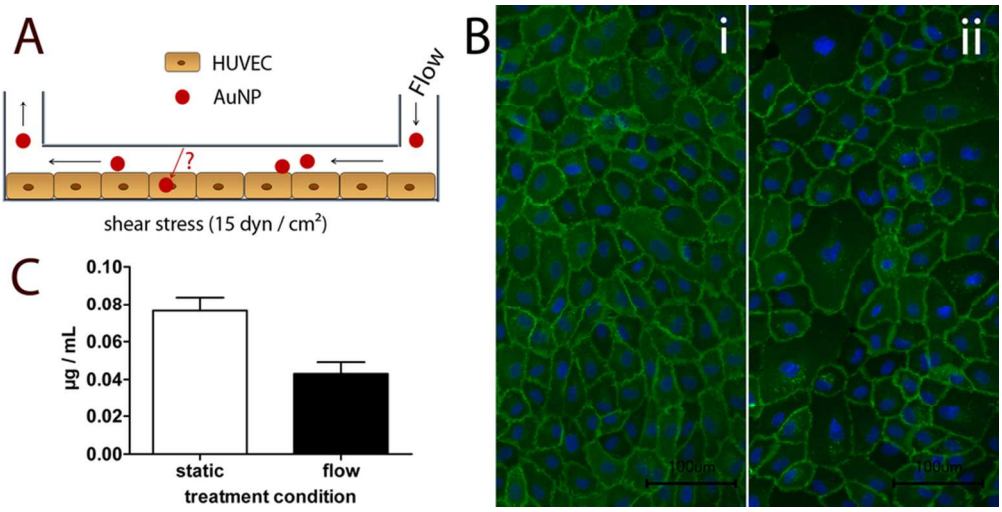

Figure 2. Treatment of HUVEC with 20 nm PEGylated gold nanoparticles under flow culture conditions. (A) Cartoon of the flow culture model system (15 dyn / cm²). (B) Immunofluorescent images of HUVEC under flow culture conditions without (i) or exposed to gold nanoparticles (ii). Staining of CD31 (green) expressed in HUVEC, nuclei in blue, scale bars: 100 µm. (C) Quantification of internalized gold in HUVEC under static or flow culture conditions determined using ICP-OES (n = 6).

85x42mm (300 x 300 DPI)

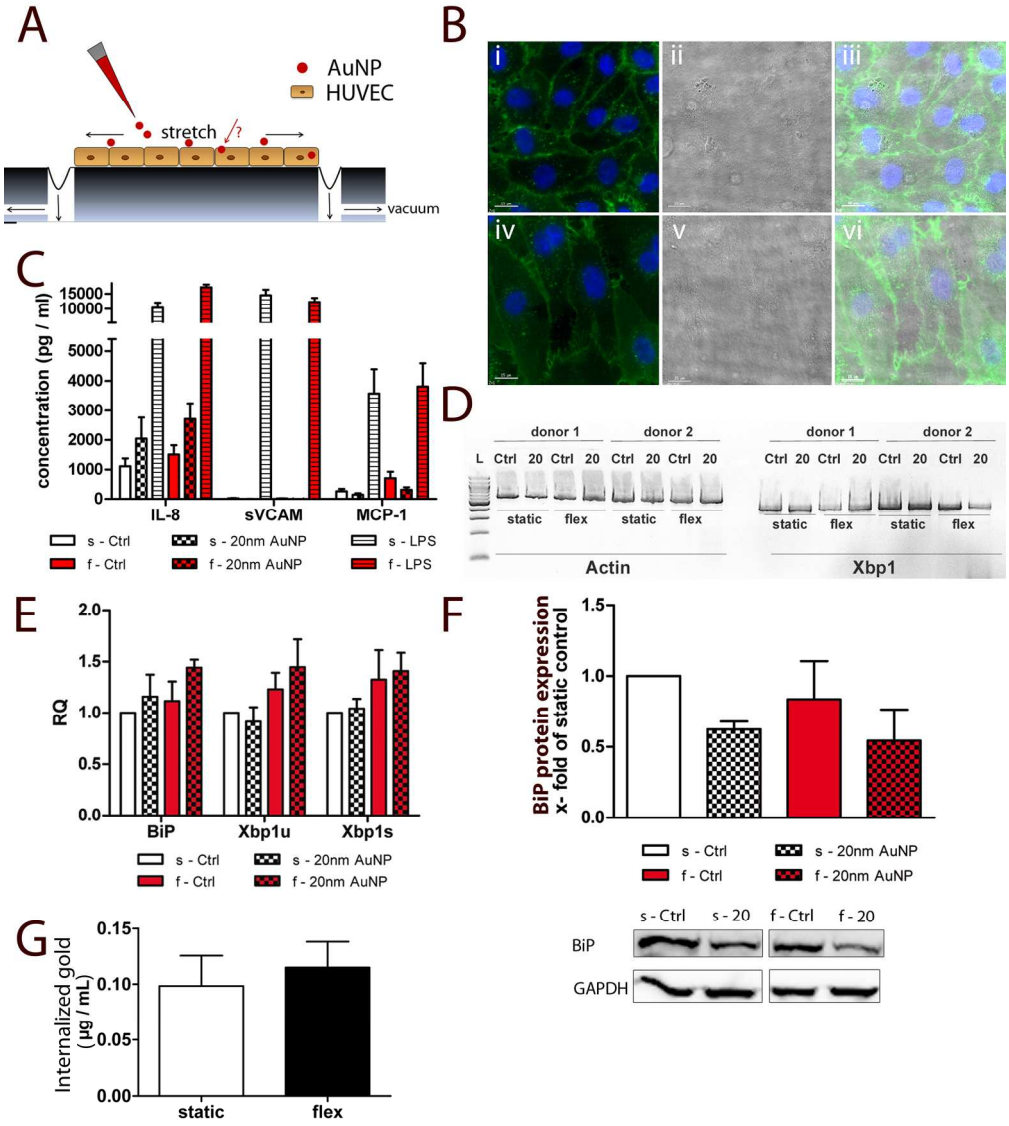

Figure 3. Impact of PEGylated AuNPs on HUVEC cultured under physiological stretch conditions. (A) Cartoon of the stretch model system (5 % cyclic stretch, 1 Hz). (B) Immunofluorescent images of HUVEC exposed to gold nanoparticles under static (i – iii) or stretch (iv – vi) culture conditions. Staining of CD31 (green) expressed in HUVEC (i + iv) and DIC images (ii + v); overlays in (iii) and (vi). Scale bars: 15 µm. (C) Secretion of interleukin-8 (IL-8), soluble vascular cell adhesion molecule (sVCAM), and monocyte chemoattractant protein-1 (MCP-1) after AuNP exposure under static (s) or stretch/flex (f) culture conditions measured by ELISA. LPS treatment was used as a positive control (n = 3-6). (D) PCR detecting spliced and unspliced Xbp1 mRNA via separation using a 3 % agarose gel. Actin was used as reference gene. (E) Quantitative real-time PCR for investigation of BiP, unspliced (Xbp1u) and spliced (Xbp1s) Xbp1 mRNA expression. Results are depicted as relative quantification (RQ) (n=2). (F) Quantification of BiP expression on protein level detected by Western Blot shown as X-fold change of static control (n=4). (G) Quantification of internalized gold in HUVEC under static or stretch culture conditions determined using ICP-OES (n=3).

192x216mm (300 x 300 DPI)

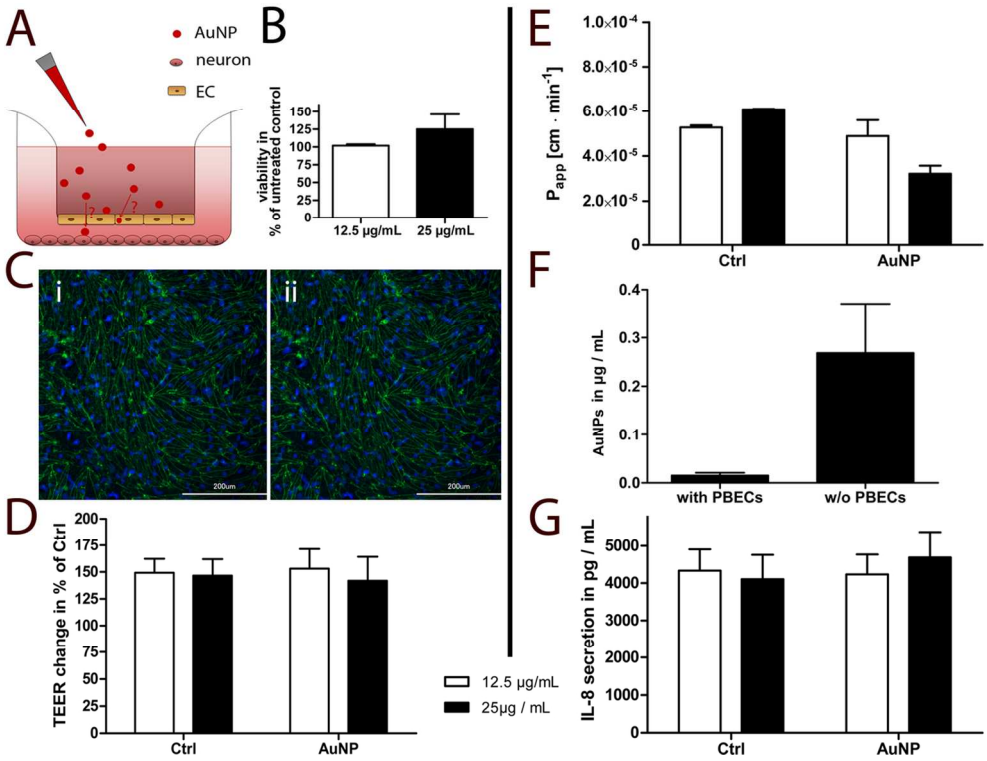

Figure 4. Assessment of the impact of 20 nm PEGylated AuNPs on endothelial cells forming the blood-brain barrier.

(A) Cartoon of the blood-brain barrier co-culture model. (B) The MTS-Assay was used to determine cell viability after 24 hours of exposure to PEGylated AuNPs and the acquired data were normalized to the untreated control expressed in % (n = 3 - 4). (C) Immunofluorescence staining of claudin-5 proteins (green) expressed in PBEC without PEGylated AuNPs (i) or after PEGylated AuNPs treatment (ii). Nuclei in blue, scale bars: 200 µm. (D) Transendothelial electrical resistance (TEER) was measured before and after the exposure to gold nanoparticles for 24 hours. Ctrl was treated with the corresponding volume of diluent. Data represent the mean ± standard deviation of four experiments. Cells with at least 170 Ohm x cm² were used (n = 4 - 5). (E) To ensure the tightness of the barrier during the treatment with PEGylated AuNPs, the permeability coefficient of sodium fluorescein was simultaneously determined (n = 2). (F) Quantification of transported gold across the PBEC barrier using ICP-OES (n = 3). (G) Secretion of interleukin-8 from PBECs during PEGylated AuNP treatment was compared to the untreated control (n = 2 - 6).

128x96mm (300 x 300 DPI)

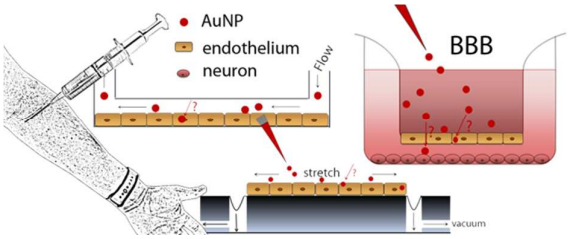

The use of physiological cell cultures as screening platforms helps to determine potential nanomaterial toxicity prior to in vivo experiments.